Fermi Surface of Metallic V_{2}O_{3} from Angle-Resolved Photoemission: Mid-level Filling of e_{g}^{π} Bands

I. Lo Vecchio, J. D. Denlinger, O. Krupin, B. J. Kim, P. A. Metcalf, S. Lupi, J. W. Allen, and A. Lanzara

Phys. Rev. Lett. **117**, 166401 — Published 11 October 2016

DOI: 10.1103/PhysRevLett.117.166401

Angle resolved photoemission study of V_2O_3: the mystery lives on

I. Lo Vecchio,[1,*] J. D. Denlinger,[2,*] O. Krupin,[2] B. J. Kim,[3] P. Metcalf,[4] S. Lupi,[5] J. W. Allen,[6] and A. Lanzara[1,7,†]

[1]*Materials Sciences Division, Lawrence Berkeley National Laboratory, Berkeley, California 94720, USA*
[2]*Advanced Light Source, Lawrence Berkeley National Laboratory, Berkeley, California 94720, USA*
[3]*Max-Planck-Institut fur Festkörperforschung, Heisenbergstr. 1, D-70569 Stuttgart, Germany*
[4]*Department of Physics, Purdue University, West Lafayette, Indiana 47907, USA*
[5]*CNR-IOM and Dipartimento di Fisica, Università di Roma "Sapienza", I-00185 Rome, Italy*
[6]*Randall Laboratory of Physics, University of Michigan, Ann Arbor, Michigan 48109, USA*
[7]*Department of Physics, University of California Berkeley, Berkeley, California 94720, USA*

Using angle resolved photoemission spectroscopy (ARPES) we report the first band dispersions and distinct features of the bulk Fermi surface (FS) in the paramagnetic metallic phase of the prototypical metal-insulator transition material V_2O_3. Along the c-axis we observe both an electron pocket and a triangular hole-like FS topology, showing that both V $3d$ a_{1g} and e_g^π states contribute to the FS. These results challenge the existing correlation-enhanced crystal field splitting theoretical explanation for the transition mechanism and pave the way for the solution of this mystery.

PACS numbers: 79.60.-i,71.27.+a,71.30.+h

Since its seminal report in 1969 [1–3], the metal-insulator transition (MIT) in the alloy system $(V_{1-x}Cr_x)_2O_3$ has stood as a mystery for many decades. For x=0 and with decreasing temperature (T) there is a transition from a paramagnetic metal (PM) to an antiferromagnetic insulator (AFI). With increasing x the AFI phase persists but the PM phase gives way to a paramagnetic insulator (PI) along an (x, T) line terminating at higher T in a critical point. The initial identification of the latter transition as the long sought experimental example of the Mott MIT [4] inherent in the one-band Hubbard model was quickly challenged [5] on the grounds that the complexity of the actual multi-orbital electronic structure must be essential for the transition. This complexity consists of four V^{3+} ions per rhombohedral unit cell with each ion having two $3d$ electrons to distribute in the two lowest energy trigonal crystal field split $3d$ states, an orbital singlet a_{1g} and an orbital doublet e_g^π. Scenarios for reducing this complexity back to a one-band model [6] were eventually abandoned after X-ray absorption spectroscopy (XAS) showed that the V^{3+} ions are in a Hund's rule S=1 state and that both the e_g^π and a_{1g} states are always occupied, albeit with different occupation ratios $e/a(=e_g^\pi{:}a_{1g})$ in the three phases [7].

The advent of dynamic mean field theory (DMFT) [8] combined [9] with band structure from density functional theory (DFT), supported by bulk sensitive angle integrated photoemission spectra for $(V_{1-x}Cr_x)_2O_3$ [10, 11], gave the first real hope that the mystery could be solved within a realistic multi-orbital calculation. Indeed a series of DFT+ DMFT studies in the first decade of this century [12–14] gradually coalesced around a narrative in which the MIT is enabled by a strong many-body enhancement of the trigonal crystal field splitting and thus the orbital polarization of the quasi-particle (QP) bands based on the e_g^π and a_{1g} states. In 2007 the claim in Ref. [14] "to have demystified the nature of the metal-insulator transition in V_2O_3" seemed well justified by the consensus. The study suggested that in the PM phase the Fermi surface (FS) is formed entirely from an a_{1g} QP band, while all the e_g^π QP bands lie entirely below the Fermi energy, E_F, a scenario consistent with electron counting only by virtue of QP weights sufficiently reduced from 1 and the concomitant presence of the lower and upper Hubbard bands below and above E_F, respectively [15]. This strongly polarized and strongly correlated situation brings the PM phase to the very brink of the MIT and the opening of a complete e_g^π - a_{1g} gap. Since then however, technical advances in DMFT aimed at achieving full charge self-consistency find much reduced orbital polarizations [16, 17], implying that what had seemed to be a finished narrative might actually be far from the true implication of DMFT for this problem.

All this detailed DMFT effort for V_2O_3 has been conducted without any guidance whatsoever from experimental k-resolved information on the QP band structure, i.e. no angle resolved photoemission spectroscopy (ARPES). In this Letter we report the first such ARPES data for the PM phase. We find that both a_{1g} and e_g^π contribute to the FS, with E_F cutting roughly through the center of the e_g^π manifold, i.e. a much weaker orbital polarization. Our results reveal the PM phase electronic structure and suggest that the correlation-enhanced crystal field splitting plays a less important role in driving the MIT than was previously thought. We find some agreement with recent fully charge self-consistent DFT+DMFT calculations, thus demonstrating that this could be the way to solve the V_2O_3 mystery.

Flat (0001) and (1000) surfaces of V_2O_3 suitable for ARPES measurements were prepared by annealing polished Laue-oriented single crystals to 750°C in a 10^{-6} Torr oxygen partial pressure resulting in 1×1 surface order measured by low energy electron diffraction. Also,

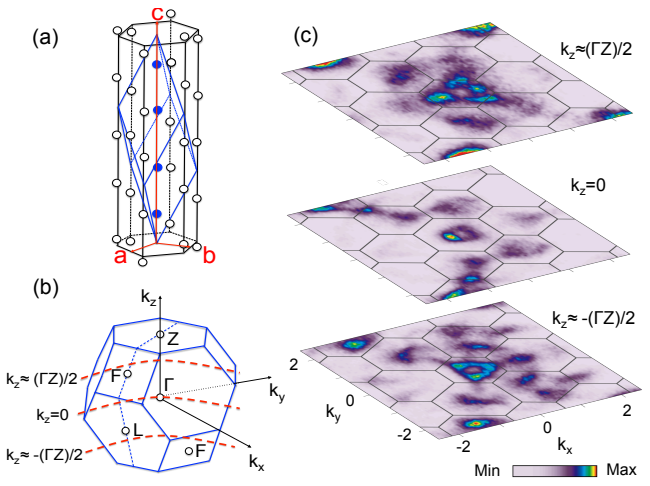

FIG. 1: (a) Rhombohedral primitive cell containing two V_2O_3 formula units (four blue V atoms), surrounded by the non-primitive hexagonal unit cell. The red hexagonal unit vectors measure a=4.94 Å and c=13.99 Å. (b) Brillouin zone for the rhombohedral unit cell of V_2O_3 paramagnetic metallic phase. (c) Electronic structure of a V_2O_3 (0001) polished single crystal along normal emission for T=200 K. Wide Fermi surface slices in the plane at the upper half BZ height (360 eV); in the Γ plane (320 eV), k_z= 9.5 Å^{-1} but labeled as k_z= 0 for simplicity; and in the plane at the lower half BZ height (280 eV), as indicated by dashed curves in (b).

room temperature blade cleaving of millimeter sized (0001)-oriented single crystals revealed similar data as for polished single crystals, but with less reproducibility of spectral clarity due to spatial variations [18]. The ARPES measurements were performed using the 2009 configuration of Beamline 7.0 of the Advanced Light Source in Berkeley utilizing photon energies from 80 eV to 900 eV and a beam spot-size of 50×50 μm. Data were acquired using a Scienta R4000 hemispherical electron analyzer with the sample placed in a vacuum better than 1×10^{-10} Torr. The transport MIT transition temperature for these samples is T_{MIT}=165 K with a hysteresis of <10 K. Thus the measurements were taken at T=200 K in order to be fully in the PM phase [19].

Fig. 1(a) shows the vanadium atom only crystal structure of V_2O_3 with two unit cell representations. The primitive rhombohedral unit cell contains two formula units (four solid blue circles along the c-axis) while the non-primitive hexagonal unit cell contains six formula units and a c-axis notation of (0001). Fig. 1(b) shows the corresponding reciprocal space rhombohedral Brillouin zone with high symmetry point labeling. Fig. 1(c) presents the first ARPES result of three constant energy maps (k_x-k_y) of the Fermi-edge intensity acquired for different values of k_z perpendicular to the (0001) surface (accesed by varying the photon energy between 280 and 360 eV). The k_z locations [20] of the maps relative to the bulk BZ correspond to k_z=9.5 Å^{-1} Γ-plane, and half-way between Γ and Z (k_z=±ΓZ/2), as shown schematically with dashed arc lines in Fig. 1(b). In the Γ-plane, a nearly six-fold intensity pattern is observed in the first and second BZs, whereas at k_z=±ΓZ/2 an overall three-fold intensity pattern is evident with a strong intensity triangular-like contour in the first BZ. The directional pointing of the triangular FS intensity is observed to reverse in the maps above and below the Γ-plane. This reversal is consistent with the symmetry of the bulk BZ and provides strong evidence for the bulk origin of these states.

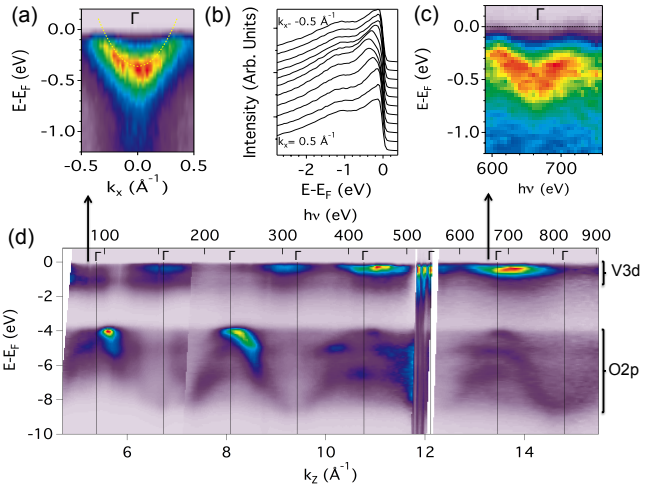

FIG. 2: Angle dependent Γ point electron pocket dispersion (a) image and (b) stack plot measured at hν=88 eV for a (1000) surface. (c) Photon dependent Γ point electron pocket measured at hν=670 eV for the (0001) surface. (d) V_2O_3 (0001) photon energy scan along normal emission, highlighting V 3d intensities down to -2 eV and O 2p bands dispersing between -4 eV and -8 eV. Vertical lines indicate locations of Γ points along the c-axis.

Fig. 2 shows the electronic structure for the (0001) and (1000) surfaces. Panel (d) shows the energy dispersion as a function of the out-of-plane momentum k_z for normal emission with respect to the (0001) surface (i.e. along the c axis), over multiple Brillouin zones, by varying the photon energy over a 800 eV wide energy range [20]. The wide binding energy scale shows both the dispersions of the O 2p bands between 4 and 8 eV and the V 3d states below 1 eV. The Γ points (Brillouin zone center) for each BZ are indicated by a vertical line. The photon dependence is interrupted between 510-560 eV due to strong variations from the V L- and oxygen K-absorption edges. Both the O 2p band dispersion and the V 3d states near E_F show a spectral intensity variation with half unit-cell periodicity. These indicate that the half unit-cell is the primary c-axis periodicity of the potential felt by oxygen orbitals. At more surface sensitive lower photon energies

the O $2p$ band dispersion resembles a single 4 eV wide sinusoidal band whereas at higher photon energy the increasing bulk-sensitivity results in greater partitioning of the O $2p$ states into sub-bands [16].

Fig. 2(c) shows an expanded zoom of the V $3d$ dispersion around 670 eV, showing an electron pocket centered at Γ. The reduced visibility of the vanadium states at lower photon energy may be related to the existence of a structural relaxed and/or vanadyl surface termination [21] resulting in a non-metallic half-unit cell surface and a surface dead layer[22]. Nevertheless, electron pockets can be observed at low photon energy Γ-points for the orthogonal (1000) polished surface with the c-axis in plane and the unit cell b-vector perpendicular to the surface. We conjecture that no such insulating dead layer exists for this (1000) surface. Fig 2(a) shows the Γ-point electron pocket for this surface measured at 88 eV which allows finer quantification of the electron dispersion to be 0.4 eV deep and 0.75 Å^{-1} wide. The Fig. 2(b) stack plot of spectra illustrates the relative amplitude of the dispersing component of electron pocket states at 88 eV relative to a broad non-dispersing component of the QP peak and relative to the incoherent band between 0.5 eV and 1.5 eV. The presence of a non-dispersive component in the metallic QP energy region is in part why ARPES of V_2O_3 has been such a challenging task. Also it produces the visual artifact of the dispersion peak (in color intensity images) not reaching the Fermi level, whereas the metallic dispersion to E_F is confirmed by momentum distribution curves cuts of the data set(s).

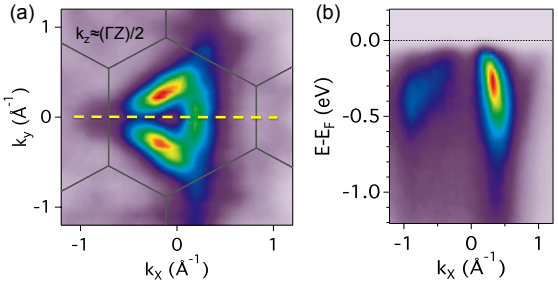

FIG. 3: (a) Triangular feature measured at 180 eV showing three arc-like pieces converging at the corners of the triangle. (b) Hole-like energy dispersion cut through the triangular feature as indicated by the yellow dashed line in panel (a).

The Fermi contour at k_z=ΓZ/2 is shown in Fig. 3(a). Data are taken at a lower photon energy (hν=180 eV) than that in Fig. 1. The overall contour resembles a triangular like shape with open tips, thus suggesting three arc-like features. A clear hole-like dispersion is visible in the energy distribution curve cut in Fig. 3(b) corresponding to the dashed line in panel (a). The Fermi velocity is 1.63 eV-Å. redThis FS feature is stable with small percentages of doping within the metallic phase, as indicated by data taken on $(V_{0.988}Cr_{0.012})_2O_3$ and $(V_{0.955}Ti_{0.045})_2O_3$ (not shown). The very existence of this triangular FS contour halfway between Γ and Z strongly contradicts the DFT + DMFT calculation reported in [14] in which only a single zone-centered a_{1g} electron FS is remaining while the top of the e_g^π states is pushed fully below E_F. Moreover the predicted depth of the a_{1g} electron band at Γ is shallower than the experimental ARPES value of 0.4 eV [23].

We have explored constant energy contours of various non-magnetic DFT+U calculations, under the assumption that the DMFT energy renormalization, quasiparticle weight reduction and spectral weight redistribution, absent in DFT, does not radically change the shape of the QP band dispersions. Fig. 4(a) and (b) show the 3D Fermi surface of a DFT+U (6.5 eV) calculation [24] with constrained zero moment and a k_z=0.3 Å^{-1} (0.45·Γ-Z) "spectral" image cut of Lorentzian-broadened Fermi-energy contours. The calculation exhibits three-fold symmetric electron (e) and hole (h) sheets pointing upwards away from the center Γ-Z axis towards the square and hexagonal zone-boundary faces, respectively. The spectral weight of the inner edges of the electron sheets, containing vertical edges along the c-axis, are strongly enhanced with k_z-broadening [23] relative to the highly k_z-dispersing parts of the electron or hole sheets. These three-fold arcs give rise to the appearance of an open-tipped triangular Fermi surface that is very similar in size and shape to that of the ARPES measurement shown in Fig. 3(a). The increased U value relative to that in earlier DMFT calculations[14] produced the best agreement with the experimental results and is generally consistent [23] with the values used in more recent DMFT calculations [16, 17, 25].

The band dispersion for the DFT+U calculation is shown in Fig. 4(c). The lowest of 4 a_{1g} bands crosses E_F approximately half-way along Γ-Z and the other 3 bands are unoccupied. The zone-centered electron sheet

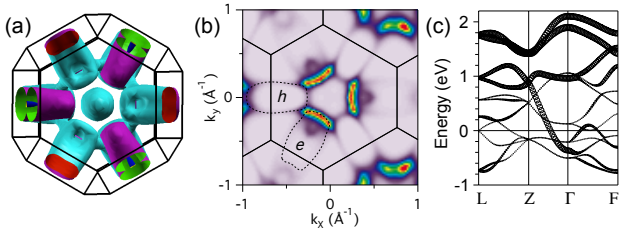

FIG. 4: (Color Online) (a) Top view of the theoretical Fermi surface of a non-magnetic DFT+U (6.5 eV) calculation including both electron (blue) and hole (purple) sheets. (b) k_z=0.3 Å^{-1} image cut of Lorentzian k-broadened Fermi-edge contours. (c) V $3d$ band structure for the same calculation with highlighting of the a_{1g} orbital character (fat line).

corresponding to this partially occupied a_{1g} band is visible in the 3D Fermi surface in Fig. 4(a). The plot of band dispersions also clearly shows that E_F then cuts in the middle of the e_g^π bands. It is very encouraging that two more recent k-resolved DFT + DMFT calculations [16, 17] incorporating full charge self-consistency predict e_g^π QP bands above and crossing E_F corresponding to less than half-filling of the e_g^π QP states [23]. Our experimental result supports this scenario and does not support the earlier filled e_g^π QP band scenario [14] in which the PM phase is at the threshold of the formation of an a_{1g}-e_g^π insulator gap at E_F.

The mid-filling of the e_g^π QP states in the PM phase, as opposed to being at the brink of an a_{1g}-e_g^π direct gap, challenges theory anew as to how the lattice constant or magnetic ordering perturbations of the PI and AFI phases are able to open an insulating gap. A possible answer may lie with new charge self consistent but non-k-resolved GGA + DMFT calculations that find the MIT to be driven by a strong orbital selective renormalization featuring the e_g^π QP weight going to zero [25]. A calculation of k-resolved QP bands for comparison to our data would be required to more fully evaluate this line of study. Recent hard x-ray photoemission and absorption experiments have provided additional MIT model constraints on the variation of U between the metal and insulating phases [26] and on the different variation of the orbital occupancies for the pressure-induced PI phase [27] as compared to the Cr-doping and temperature induced PI phases. Thus the mystery of the MIT lives on.

In conclusion we have reported experimental electron- and hole-like band dispersions in the metallic phase of V_2O_3 at specific k-locations in the bulk Brillouin zone and with distinct Fermi surface topologies. We associate them with a_{1g} and roughly half filled e_g^π QP bands, thus supporting the scenario of partially filled e_g^π states, in disagreement with previously reported k-resolved DMFT calculations that described the metallic phase at the brink of a MIT driven by correlation-enhanced crystal field splitting . These results are a major new spectroscopic contribution to the long sought goal of a final and complete understanding of the $(V_{1-x}Cr_x)_2O_3$ MIT paradigm.

We gratefully acknowledge theoretical advice and stimulating discussions with Byung Il Min, Richard Martin and especially Frank Lechermann. This work was supported by the National Science Foundation grant number DMR-1410660. The Advanced Light Source is supported by the U.S. Department of Energy.

* These two authors contributed equally to this work.
† emailaddress:alanzara@lbl.gov

[1] D. B. McWhan, T. M. Rice, and J. P. Remeika, Phys. Rev. Lett. **23**, 1384 (1969).
[2] D. B. McWhan and J. P. Remeika, Phys. Rev. B **2**, 3734 (1970).
[3] D. B. McWhan, A. Menth, J. P. Remeika, W. F. Brinkman, and T. M. Rice, Phys. Rev. B **7**, 1920 (1973).
[4] N. F. Mott, Rev. Mod. Phys. **40**, 677 (1968).
[5] J. B. Goodenough, Ann. Rev. Phys. **1**, 101 (1971).
[6] C. Castellani, C. R. Natoli, and J. Ranninger, Phys. Rev. B **18**, 4945 (1978).
[7] J.-H. Park, L. H. Tjeng, A. Tanaka, J. W. Allen, C. T. Chen, P. Metcalf, J. M. Honig, F. M. F. de Groot, and G. A. Sawatzky, Phys. Rev. B **61**, 11506 (2000).
[8] A. Georges, G. Kotliar, W. Krauth, and M. J. Rozenberg, Rev. Mod. Phys. **68**, 13 (1996).
[9] K. Held, Adv. Phys. **56**, 829 (2007).
[10] S.-K. Mo, J. D. Denlinger, H.-D. Kim, J.-H. Park, J. W. Allen, A. Sekiyama, A. Yamasaki, K. Kadono, S. Suga, Y. Saitoh, T. Muro, P. Metcalf, G. Keller, K. Held, V. Eyert, V. I. Anisimov, and D. Vollhardt, Phys. Rev. Lett. **90**, 186403 (2003).
[11] S.-K. Mo, H.-D. Kim, J. D. Denlinger, J. W. Allen, J.-H. Park, A. Sekiyama, A. Yamasaki, S. Suga, Y. Saitoh, T. Muro, and P. Metcalf, Phys. Rev. B **74**, 165101 (2006).
[12] K. Held, G. Keller, V. Eyert, D. Vollhardt, and V. I. Anisimov, Phys. Rev. Lett. **86**, 5345 (2001).
[13] M. S. Laad, L. Craco, and E. Müller-Hartmann, Phys. Rev. Lett. **91**, 156402 (2003).
[14] A. I. Poteryaev, J. M. Tomczak, S. Biermann, A. Georges, A. I. Lichtenstein, A. N. Rubtsov, T. Saha-Dasgupta, and O. K. Andersen, Phys. Rev. B **76**, 085127 (2007).
[15] As a rough illustration that considers only the e_g^π states which account for very nearly all 8 of the electrons per unit cell, i.e. neglects the small fraction in the a_{1g} QP bands, it is consistent that the e_g^π QP weight Z is 0.2 and that the division of the k-integrated spectral weight below E_F is roughly equal between the QP bands and the lower Hubbard band.
[16] D. Grieger and F. Lechermann, Phys. Rev. B **90**, 115115 (2014).
[17] X. Deng, A. Sternbach, K. Haule, D. N. Basov, and G. Kotliar, Phys. Rev. Lett. **113**, 246404 (2014).
[18] H. Fujiwara, T. Kiss, Y. K. Wakabayashi, Y. Nishitani, T. Mori, Y. Nakata, S. Kitayama, K. Fukushima, S. Ikeda, H. Fuchimoto, Y. Minowa, S.-K. Mo, J. D. Denlinger, J. W. Allen, P. Metcalf, M. Imai, K. Yoshimura, S. Suga, T. Muro, and A. Sekiyama, J. Synchrotron Rad. **22**, 776 (2015).
[19] S. Lupi, L. Baldassarre, B. Mansart, A. Perucchi, A. Barinov, P. Dudin, E. Papalazarou, F. Rodolakis, J. -P. Rueff, J. -P. Itie, S. Ravy, D. Nicoletti, P. Postorino, P. Hansmann, N. Parragh, A. Toschi, T. Saha-Dasgupta, O. K. Andersen, G. Sangiovanni, K. Held, and M. Marsi, Nat. Commun. **1**, 105 (2010).
[20] At normal emission ($k_{||}$=0) and lower photon energy k_z in Å is related to the photon energy in eV by k_z=0.512$\sqrt{(h\nu - \phi + V_0)}$, where ϕ=4.5 eV is the work function of the analyzer and V_0=14 eV is the so-called inner potential. At higher photon energy this basic relation has been modifed to include quantitatively important effects of the photon momentum.
[21] F. E. Feiten, J. Seifert, J. Paier, H. Kuhlenbeck, H. Winter, J. Sauer, and H.-J. Freund, Phys. Rev. Lett. **114**,

216101 (2015).
[22] G. Borghi, M. Fabrizio, and E. Tosatti, Phys. Rev. Lett. **102**, 066806 (2009).
[23] See Supplementary Materials for k-resolved DMFT comparison and other details of all the various calculations, including band occupations and the effect of k_z broadening.
[24] P. Blaha, K. Schwarz, G. K. H. Madsen, D. Kvasnicka, and J. Luitz, WIEN2k, (Karlheinz Schwarz, Techn. Universitat Wien, Austria, 2001).
[25] I. Leonov, V. I. Anisimov, and D. Vollhardt, Phys. Rev. B **91**, 195115 (2015).
[26] H. Fujiwara, A. Sekiyama, S.-K. Mo, J. W. Allen, J. Yamaguchi, G. Funabashi, S. Imada, P. Metcalf, A. Higashiya, M. Yabashi, K. Tamasaku, T. Ishikawa, and S. Suga, Phys. Rev. B **84**, 075117 (2011).
[27] F. Rodolakis, P. Hansmann, J.-P. Rueff, A. Toschi, M. W. Haverkort, G. Sangiovanni, A. Tanaka, T. Saha-Dasgupta, O. K. Andersen, K. Held, M. Sikora, I. Alliot, J.-P. Itié, F. Baudelet, P. Wzietek, P. Metcalf, and M. Marsi Phys. Rev. Lett **104**, 047401 (2010).